European Journal of Pharmaceutical Sciences 159 (2021) 105731

Contents lists available at ScienceDirect

European Journal of Pharmaceutical Sciences

journal homepage: www.elsevier.com/locate/ejps

# Design, synthesis and antihypertensive evaluation of novel codrugs with combined angiotensin type 1 receptor antagonism and neprilysin inhibition

Alessandra Mascarello [1,*], Hatylas Azevedo [1], Marcos Antonio Ferreira Junior [1], Eloisa Eriko Ishikawa, Cristiano Ruch Werneck Guimarães

*Aché Laboratórios Farmacêuticos, Guarulhos, São Paulo 07034-904, Brazil*

ARTICLE INFO

*Keywords:*
Antihypertensive
Neprilysin
Angiotensin
Codrug
Prodrug
Losartan

ABSTRACT

The multifactorial etiology of hypertension has promoted the research of blood pressure-lowering agents with multitarget actions to achieve better clinical outcomes. We describe here the discovery of novel dual-acting antihypertensive codrugs combining pharmacophores with angiotensin type 1 (AT1) receptor antagonism and neprilysin (NEP) inhibition. Specifically, the codrugs combine the AT1 antagonists **losartan** or its carboxylic acid active metabolite (**E-3174**) with selected monocarboxylic acid NEP inhibitors through a cleavable linker. The resulting codrugs exhibited high rates of *in vitro* conversion into the active molecules upon incubation with human/rat liver S9 fractions and *in vivo* conversion after oral administration in rodents. Moreover, the acute effects of one of the designed codrugs (**3b**) was confirmed at the doses of 10, 30 and 60 mg/kg p.o. in the spontaneous hypertensive rat (SHR) model, showing better antihypertensive response over 24 hours than the administration of an equivalent fixed-dose combination of 15 mg/kg of **losartan** and 14 mg/kg of the same NEP inhibitor used in **3b**. The results demonstrate that the codrug approach is a plausible strategy to develop a single molecular entity with combined AT1 and NEP activities, aiming at achieving improved pharmacokinetics, efficacy and dosage convenience, as well as reduced drug-drug interaction for hypertension patients. In addition, the developability of the codrug should be comparable to the one of marketed AT1 antagonists, most of them prodrugs, but bearing only the AT1 pharmacophore.

## 1. Introduction

Primary hypertension affects more than 1 billion people worldwide (World Health Organization, 2019). Despite the availability of many marketed drugs, eighty percent of the hypertensive patients display a suboptimal blood pressure control. Hence, these patients could benefit from combination therapies to prevent more severe cardiovascular diseases. Multitarget drugs can provide greater antihypertensive potential than using high doses of a monotherapy, due to the synergistic effects of modulating distinct pathways (Guerrero-García& Rubio-Guerra, 2018).

The renin-angiotensin-aldosterone (RAA) and the natriuretic peptide (NP) systems play a role in hypertension (Braunwald, 2015; Hubers and Brown, 2016). Angiotensin II (Ang II) is the major effector of the RAA axis, acting via the AT1 receptor to promote vasoconstriction, aldosterone release and water retention. Several AT1 receptor blockers (ARBs), also known as sartans, have been developed (Miura et al., 2011). They are formed by a biphenyl-methyl backbone combined with one or two acidic groups like tetrazole and carboxylic acid, which are required for potency but lead to poor oral drug bioavailability, especially with two ionizable acidic groups. Accordingly, some of the marketed ARBs are inactive prodrugs, such as candesartan cilexetil and olmesartan medoxomil, that are converted into their active forms in the plasma (Barreras and Gurk-Turner, 2003).

**Losartan** is an ARB that has an oral bioavailability of 33% due to its conversion to the 10-fold more potent metabolite **E-3174** (Fig. 1), formed by oxidation of the C5-hydroxymethyl on the imidazole ring

*Abbreviations:* ANOVA, analysis of variance; AUC, area under the curve; DBP, diastolic blood pressure; DMSO, dimethyl sulfoxide; G6P, glucose 6-phosphate; G6PDH, glucose-6-phosphate dehydrogenase; HIS9, human intestine S9; HLS9, human liver S9; HR, heart rate; MAP, mean arterial pressure; NADP, nicotinamide adenine dinucleotide phosphate; NEP, neprilysin; NEPi, neprilysin inhibitor; PAPS, 3'-phosphoadenosine-5'-phosphosulphate; PK, pharmacokinetics; SBP, systolic blood pressure; SD, Sprague Dawley; S.E.M., standard error of the mean; SHR, spontaneous hypertensive rat; UDPGA, uridinediphosphateglucuronic acid.

* Corresponding author at: Aché Laboratórios Farmacêuticos, Rodovia Presidente Dutra Km 222,2. Guarulhos, São paulo 07034-904, Brazil
*E-mail address:* alessandra.mascarello@ache.com.br (A. Mascarello).
[1] First co-authors, contributed equally to this work.

https://doi.org/10.1016/j.ejps.2021.105731
Received 15 December 2020; Received in revised form 15 January 2021; Accepted 19 January 2021
Available online 23 January 2021

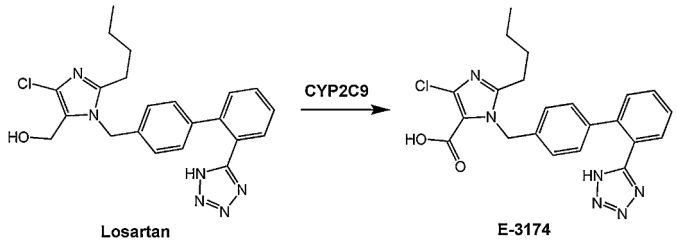


**Fig. 1.** Conversion of losartan to its more active carboxylic acid metabolite (E-3174) by the CYP2C9 enzyme.

(Sica et al., 2005). The terminal half-lives of **losartan** and **E-3174** are 2 and 6-9 hours, respectively. **Losartan** produces a biphasic inhibition of the Ang II pressor response, with a short peak inhibition followed by a gradual decrease over 3 hours (Wong et al., 1990a), suggesting that **E-3174** could participate in the lasting action of **losartan** (Christen et al., 1991). The cytochrome P450 2C9 (CYP2C9) mediates the oxidation of **losartan** to **E-3174,** and CYP2C9 variants confer clinical differences in **losartan** metabolism (Yasar et al., 2002) and antihypertensive effects (Joy et al., 2009). The dependence on CYP2C9 metabolism is not desirable from a drug-drug interaction perspective, since the concomitant use of CYP2C9 substrates/inhibitors may lead to insufficient **E-3174** levels and 24-hour blood pressure control (Daly et al., 2017) . Moreover, the CYP2C9-mediated formation of **losartan** adducts (Iwamura et al., 2011) has been involved in drug-induced liver injury (Patti et al., 2019).

The NP system is consisted of peptides that are released by mechanical stretching of the atria and left ventricle, inducing natriuresis, diuresis, and vasodilation (Bavishi et al., 2015). These peptides are inactivated by the metalloprotease neprilysin (NEP), which has stimulated the exploration of NEP inhibitors such as sacubitrilat, phosphoramidon and candoxatrilat to increase circulating levels of NPs. A series of mono and dicarboxylic acid glutaramides based on candoxatrilat has shown good potency and oral absorption in rats (Maw et al., 2006; Pryde et al., 2006; Pryde et al., 2007).

The simultaneous modulation of the RAA and NP systems via AT1 antagonism and NEP inhibition can synergistically promote hemodynamic effects (Maslov et al., 2019). Accordingly, the combination of an ARB and a NEP inhibitor in a single pharmaceutical form has been explored in the clinic. LCZ696 (Entresto®) is a first-in-class, fixed-dose AT1 antagonist-NEP inhibitor combination, that was approved by the FDA for the treatment of chronic heart failure. The twice daily administration of LCZ696 reduces the risk of cardiovascular complications by 20% (McMurray, 2014). LCZ696 is a non-covalently bound co-crystal of the sodium salts of sacubitril (NEP inhibitor) and valsartan (ARB) that promotes greater solubility and absorption of the parent molecules. Although co-crystals can improve solid-state forms beyond salts and polymorphs, they have several development challenges, like regulatory, manufacturing, stability and physicochemical issues. The mismatches between the p$K_a$ or solubility of the comprising drugs narrow the use of co-crystals, i.e., p$K_a$ differences greater than 1 log unit can result in salt rather than co-crystal formation (FDA, 2018), and differential solubility can yield non-stoichiometric crystal units (Thipparaboina et al., 2016). The diversity of crystal packing arrangements can also lead to complex crystal structures (Kavanagh et al., 2019). Indeed, each unit cell of LCZ696 has six sacubitril and six valsartan anionic molecules, 18 penta- and hexa-coordinated sodium cations, and 15 water molecules, with a molecular formula of $C_{288}H_{330}N_{36}O_{48}Na_{18}\bullet 15H_2O$, and weight of 5748.03 g/mol (Feng et al., 2012).

This work has explored a different approach than co-crystals to modulate the RAA and NP systems using a single molecular entity that chemically combines the pharmacophores of AT1 antagonists and NEP inhibitors into reciprocal prodrugs (also named codrugs). Codrugs are defined as two active molecules that are combined into a single molecule through a cleavable linker, which is enzymatically hydrolyzed *in vivo,* releasing the active molecules (PariseFilho et al., 2010). Codrugs are useful when a combination therapy is desirable but one of the active molecules or both show poor oral exposure as individual molecular entities. This approach is different than classical prodrugs, such as sartans, that are formed by incorporating pharmacologically inactive moieties in an active drug to improve its oral absorption. Since prodrugs are needed to deliver optimal plasma concentrations of an AT1 antagonist, why not swap the inactive moiety of sartan prodrugs by a NEP inhibitor to generate a codrug? In this way, most of the atoms would serve a more "honorable" purpose. More importantly, the codrug strategy may offer better pharmacokinetics, efficacy and reduced drug-drug interactions over sartans and even LCZ696, while keeping developability comparable to sartans, *i.e.*, much simpler and less limiting than co-crystals.

## 2. Material and methods

### 2.1. Drugs and formulation

**Losartan**, candesartan, candesartan cilexetil and sacubitrilat were purchased from Sigma-Aldrich (St. Louis, MO, USA). For the *in vitro* assays, compounds were prepared as dimethyl sulfoxide (DMSO) stock solutions and diluted in the appropriate buffers. The compounds were formulated in 5% DMSO, 10% Solutol and 85% aqueous saline solution for the *in vivo* studies.

### 2.2. Animals

Male Sprague Dawley (SD) rats and spontaneously hypertensive rats (SHR), 7-9 weeks, from Vital River (Beijing, China) were used for the *in vivo* pharmacokinetics (PK) studies. Male SHR, ~11-12 weeks, from Vital River (Beijing, China) were used for the *in vivo* efficacy study. The animals were housed in pairs at 20 – 26°C, relative humidity of 30 – 70%, 12 h artificial light and 12 h dark. Food and water were available *ad libitum*, except if stated otherwise. Animals were acclimated under these conditions for at least 3 days (PK) or 2 weeks (efficacy) before being placed on a study. All the experiments were conducted in accordance with institutional guidelines and the recommendations of the Association for Assessment and Accreditation of Laboratory Animal Care International (AAALAC), the Animal Welfare Act and the Guide for the Care and Use of Laboratory Animals. The experimental procedures were reviewed and approved by the Animal Care and Use Committee from WuXiAppTec (Shanghai, China) under the protocol number GP02-059-2018v1.0.

### 2.3. Cheminformatics analysis

A cheminformatics analysis was performed using the RDKit and the Chemistry Development Kit (CDK) nodes implemented in KNIME (University of Konstanz) to select the best NEP inhibitors (NEPi) for the design of codrugs. Specifically, the half-maximal inhibitory concentration ($IC_{50}$) and the inhibition constant ($K_i$) values of 1,039 compounds against NEP were downloaded from the ChEMBL database and converted to the negative logarithm (p$IC_{50}$ and p$K_i$, respectively). Compounds with p$IC_{50}$/p$K_i$<6.5, molecular weight >500 g/mol and logP>5 were removed from the dataset. In addition, molecules containing phosphates, hydroxamic acids or thiols were filtered out. Finally, molecules containing more than two aromatic rings, and those with two or more acid groups were also removed. The lipophilicity of the compounds was estimated using the *in silico* partition coefficient (clogP) method proposed by Mannhold et al. (2009) and implemented in the CDK node. Lipophilic ligand efficiency (LLE) values were calculated for the remaining compounds (LLE = p$IC_{50}$ – clogP) and a scatter plot was built to select compounds with both high p$IC_{50}$ (x-axis) and LLE (y-axis) values for optimal properties of the codrugs.

### 2.4. In vitro NEP inhibition

The *in vitro* NEP inhibition assay was performed using human recombinant enzyme (Anaspec, Fremont, CA, USA) and the fluorogenic peptide Mca-RPPGFSAFK(Dnp)-OH (R&D Systems, Shanghai, China), as previously described (Johnson and Ahn, 2000; Moss et al., 2020; Ruf et al., 2012). The compounds were assessed, in duplicate, in a 5-point log serial dilution within the concentration ranges 3 nM – 30 μM or 0.1 nM – 1 μM (sacubitrilat only).The compounds were incubated with the recombinant enzyme (0.1 ng/μL) for 30 min, at room temperature, in a Tris-HCl buffer (50 mM, pH 6.5). The reaction was initiated by adding the enzyme substrate (10 μM), which was then incubated for 90 min at room temperature. The fluorescence was measured using the FlexStation Microplate Reader (Molecular Devices, San Jose, CA, USA), excitation at 328 nm and emission at 393 nm.

### 2.5. Stability in liver and intestine S9

Metabolic stability studies were performed using liver and intestine S9 fractions (LS9 and IS9, respectively) from humans and SD rats, as previously described (Plant, 2004; Richardson et al., 2016). The codrugs (1 μM) were incubated with the S9 fractions (1 mg of protein/mL) for 60 min, at 37°C, with sample collection at 0, 5, 10, 20, 30 and 60 minutes. The concentrations of the parent and the active compounds of interest were quantified. The assay buffer was potassium phosphate (100 mM, pH 7.4) and the cofactors were NADP (1.3 mM), G6P (3.3 mM), G6PDH (0.4 U/mL), UDPGA (2.5 mM), PAPS (0.1 mM) and $MgCl_2$ (3.3 mM). At each time point, the stop solution (cold methanol) was added to the incubation mixture, followed by centrifugation. The peak areas corresponding to the analytes were determined by HPLC-MS/MS. The *in vitro* half-life ($t_{1/2}$) was calculated based on their disappearance rate (k, slope of the natural logarithm of concentration versus time curve) assuming first-order reaction kinetics, using the formula $t_{1/2} = 0.693/-k$.

### 2.6. Stability in aqueous buffers, simulated gastric (SGF) and intestinal fluids (SIF)

The stability of selected compounds was assessed in aqueous buffers at pH 1.1, 6.5 and 7.4, simulated gastric (SGF) and intestinal fluids (SIF). The buffers used were 75 mM phosphate buffer (pH 6.5 and 7.4) and 75 mM phosphate buffer with 6N HCl (pH 1.1). SGF (pH 1.2) consisted of NaCl (35 mM), HCl (80 mM) and pepsin (0.3%, w/v) and SIF (pH 6.8) consisted of $KH_2PO_4$ (50 mM) and pancreatin (1%, w/v). The compounds (2 μM) were incubated for 24 h in each medium, in duplicate, at 37°C, with sample collection at 0, 1, 2, 6 and 24 h. The collected samples were mixed with cold acetonitrile and analyzed by HPLC-MS/MS. The experiments were performed in duplicate. The *in vitro* half-life ($t_{1/2}$) was calculated based on the parent compound disappearance rate (k, slope of the natural logarithm of concentration versus time curve) assuming first-order reaction kinetics, using the formula $t_{1/2} = 0.693/-k$.

### 2.7. Stability in plasma

The stability of selected compounds was assessed in human and SD rat plasma. Compounds (2 μM) were incubated with the plasma for 2 h, at 37°C, in duplicate and samples were collected at 0, 10, 30, 60 and 120 min. At each timepoint, the stop solution (50:50 v/v acetonitrile/methanol) was added and the disappearance of parent test compounds and their conversion to the metabolites were quantified by HPLC-MS/MS. The *in vitro* half-life ($t_{1/2}$) was calculated based on the parent compound disappearance rate (k, slope of the natural logarithm of concentration versus time curve) assuming first-order reaction kinetics, using the formula $t_{1/2} = 0.693/-k$.

### 2.8. Aqueous kinetic solubility

Aqueous kinetic solubility was determined in a phosphate-buffered saline (PBS, pH 7.4) using the shake-flask method (Lipinski et al., 2001). Compounds were diluted in DMSO and transferred to the assay medium at the target solubility (200 μM). Samples were incubated for 24 hours under constant shake (800 rpm) at room temperature and analyzed by HPLC-MS. The experiment was performed once in duplicate.

### 2.9. Pharmacokinetic (PK) studies

The PK of selected compounds was assessed in SD and SHR rats following acute intravenous (i.v.) and oral (p.o.) administration. The animals from the p.o. groups were fasted for 12 h and then given access to food 4 h post-dose.Water was available *ad libitum*. The plasma concentrations of the parent (**losartan** and **3b**) and the active compounds of interest (**E-3174** and **1a**) were monitored over a 24-hour period after dosing and used to calculate the PK parameters. Data is reported as mean ± SEM of n = 3 animals per group.

The concentrations of the test compounds in plasma samples were determined using SCIEX Triple Quad 6500+ LC-MS/MS system with a Turbo Spray Ion Drive ionization source and a triple quadrupole analyzer. Chromatographic separation was achieved with an ACQUITY UPLC BEH C18 column (1.7 μm, 2.1 × 50 mm), a gradient of 100% solvent A to 100% solvent B (solvent A: 95:5 v/v water with 0.1% formic acid and 2 mM $NH_4HCO_2$ in Water/Acetonitrile; solvent B: 5:95 v/v water with 0.1% formic acid and 2 mM $NH_4HCO_2$ in Water/Acetonitrile) at the flow rate of 0.65 mL/min.

The oral bioavailability of the parent and active molecules were estimated using the equation below, based on the calculation described elsewhere (Guo et al., 2012; Tao et al., 2018). The dose values used in the formula were the molar equivalents of the parent compounds or active compounds in mols per kg of the animals' body weight to account for molar differences between the administered doses in mg/kg. Specifically, it is important to use molar equivalents to correctly obtain the oral bioavailability of an active molecule administered directly in the i.v. leg but as part of a codrug in the p.o. leg.

$$\text{Bioavailability } (\%) = \frac{AUC\ p.o.\ \ X\ Dose\ i.v.\ (mols\ per\ kg)}{AUC\ i.v.\ X\ Dose\ p.o.\ (mols\ per\ kg)}$$

### 2.10. Antihypertensive testing of the codrug 3b in spontaneous hypertensive rats (SHR)

The evaluation of the blood pressure-lowering effects of the codrug **3b** was performed using the SHR model (Lerman et al., 2019; Pinto et al., 1998; Wang et al., 2017). After seven days of cage habituation, rats were acclimated to the tail-cuff device (Kent Scientific Corporation) twice daily for 3 days. Animals had access to food and water *ad libitum*. To obtain a reading, the occlusion cuff was placed near the tail base, inflated, and then deflated slowly. The systolic blood pressure (SBP) was determined when the volume pressure recording cuff, placed further from the tail base, first registered a change in tail volume. The occlusion cuff continued to deflate until the inflow and outflow of blood was equalized, leading to a stable tail volume and yielding the diastolic blood pressure (DBP). Each blood pressure (BP) measuring cycle lasted 42 seconds, consisting of a 20-second measuring period followed by a 22-second refractory period.

Besides SBP and DBP, the assessed cardiovascular parameters were heart rate (HR) and mean arterial pressure (MAP). MAP was calculated as DBP + 1/3 (SBP – DBP). Animals were screened for baseline BP and only the ones displaying SBP higher than 165 mmHg were selected for the study. The rats were randomly divided into 6 groups, n = 8 per group, which were subjected to acute oral treatment with (i) vehicle, (ii-iv) **3b** at 10, 30 or 60 mg/kg, (v) **losartan** at 15 mg/kg, and (vi) the

fixed-dose combination of **losartan** at 15 mg/kg and **1a** at 14 mg/kg. The **losartan** dose in the comparator group (v) was selected considering efficacious doses previously reported in the SHR model (Gaudet et al., 1995; Wong et al., 1990b). The intermediate dose of codrug **3b** was then set at 30 mg/kg to deliver **E-3174** at an equimolar amount to **losartan** at 15 mg/kg. Two additional doses of **3b**, lower and higher than the intermediate dose (10 and 60 mg/kg), were considered. Finally, as **3b** yields **E-3174** and **1a** at an 1:1 stoichiometric ratio, the doses of **losartan** and **1a** in the combination (vi) were chosen to match equimolar amounts of the active molecules **E-3174** and **1a** upon administration of **3b** at 30 mg/kg.

The calculation of the sample size per group was determined by the power analysis based on normal distributions, using the web-based software at URL: https://www.stat.ubc.ca/~rollin/stats/ssize/n2.html, and comparing the results with reported sample sizes for ANOVA using the standardized effect size approach described in Bausell and Li (2002). The numerical assumptions for sample size calculation were (i) smallest significant BP reduction to detect of 15 mmHg, (ii) standard deviation of 10 mmHg, (iii) type I error ($\alpha$) = 5%, and (iv) type II error ($\beta$) of 20%. These assumptions were based on previous studies that tested the acute antihypertensive effects of losartan in SHR (Gaudet et al., 1995; Wong et al., 1990b).

The cardiovascular endpoints were measured at pre-dose, 1, 2, 4, 8 and 24 h after dosing. The variation ($\Delta$) of these parameters at each time point was calculated in comparison to the pre-dose values and used to estimate the parameter AUC (area under the curve) of the variation over 24 hours.

### 2.11. Statistical data analysis

The *in vitro* NEP inhibition $IC_{50}$ values were determined by the nonlinear regression analysis of the concentration-response curves using the Hill equation curve fitting in GraphPad Prism v8.0 (GraphPad Software, La Jolla, CA, USA). The PK parameters were calculated using the noncompartmental model in WinNonlin v6.3 (Certara, Princeton, NJ, USA). The statistical comparisons for the *in vivo* efficacy study were performed with GraphPad Prism v8.0 using one-way (AUC) or two-way (data over time) analysis of variance (ANOVA) followed by the Holm-Sidak post-hoc test. Statistically significant differences in SBP, DBP, MAP or HR were defined as those with multiplicity adjusted p-values lower than 0.05.

### 2.12. Chemical synthesis

All reagents and solvents were purchased from Sigma-Aldrich® and used as obtained without further purification. The progress of all reactions was monitored by analytical thin-layer chromatography, which was performed on silica-gel Silicagel 60 $F_{254}$ plates (Merck). Visualization was accomplished with UV light. Chromatographic purifications were carried out through a silica gel column using a Biotage Isolera™ Dalton 2000 automated system in gradients of dichloromethane and methanol. All $^{1}$HNMR spectra were recorded using a Bruker spectrometer (model Avance III 400 MHz or 500 MHz) at 25 °C. $^{13}$C NMR spectra were recorded using a Varian spectrometer (model Advance 125 MHz) at 27 °C. Chemical shifts ($\delta$) are given in ppm relative to $SiMe_4$ and referenced to the residual solvent signal. Coupling constants (J) are reported in Hz to the nearest 0.5. All samples were solubilized in $CDCl_3$, $CD_3OD$ or DMSO-$d_6$ and the analysis varied in time according to each sample. High Resolution (HR) mass spectrometry data (m/z) was obtained using an UHPLC Agilent 1290 Infinity with MS Agilent Q-TOF 6540 UHD Accurate-Mass system with an electrospray ionization source (Agilent Jet Stream – AJS) and Time of Flight (TOF) analyzer. Optical purity was determined by analytical HPLC analysis via comparison to racemic material. The preparation of compounds **1a, 1b, 1c** and **1d** was done as previously described (Pryde et al, 2007). The experimental details of the intermediates and final compounds **2a, 2b, 3a, 3b, 3c, 4a** and **4b** are reported in the Supporting Information (SI).

## 3. Results

### 3.1. Design of codrugs containing promoieties with AT1 antagonist and NEP inhibitory activities

The design of prodrugs requires the selection of appropriate promoieties and linkers, with several functional groups being applied to linker design, such as esters, amides, disulfide, carbonates, carbamates, oximes, phosphates, phosphonates and azo bonds (Rautio et al., 2008). Given that the most common prodrugs are formed by ester bonds that are hydrolyzed to their active carboxylic acids after gastrointestinal absorption, we decided to first explore codrugs with ester-based linkers. The compounds were designed to have **losartan** or its more active metabolite, **E-3174**, as the AT1 promoieties, and NEP inhibitors (NEPi), as the NEP promoieties, with a variety of ester linkers in between. The use of the active carboxylic acid metabolite of **losartan** (**E-3174**) in the prodrug, besides **losartan** itself, was considered so that the systemic AT1 antagonism would not be dependent on CYP2C9 conversion of **losartan** into **E-3174. E-3174** is a very interesting option as an AT1 promoiety because it is much more potent than **losartan**. In addition, **E-3174** would require a prodrug approach for oral absorption as the two ionizable acidic groups would hinder its permeability across cell membranes.

The NEPi considered as promoieties in the codrugs were selected from the literature. The dataset used in the analysis to select the best options for codrugs contained 1,039 compounds from the ChEMBL database with either $IC_{50}$ or $K_i$ NEP inhibition data available. Only compounds with potent activity ($pIC_{50}/pK_i$>6.5), low molecular weight (MW<500 g/mol) and low lipophilicity (clogP<5) were further considered. We have also filtered out NEPi with phosphates, hydroxamic acids or thiols, since these groups are less drug-like and exhibit higher potential to induce toxicity by either reactive metabolites or lack of selectivity. Molecules with two or more carboxylic acids were removed because only one of these groups could be masked in the designed codrugs. Finally, NEPi with two or more aromatic groups were excluded to keep the total number of aromatic groups in the codrugs as low as possible to mitigate poor pharmacokinetics following oral administration (Ritchie and Macdonald, 2009; Ward and Beswick, 2014).

This initial assessment has led to the identification of a set of 31 NEP

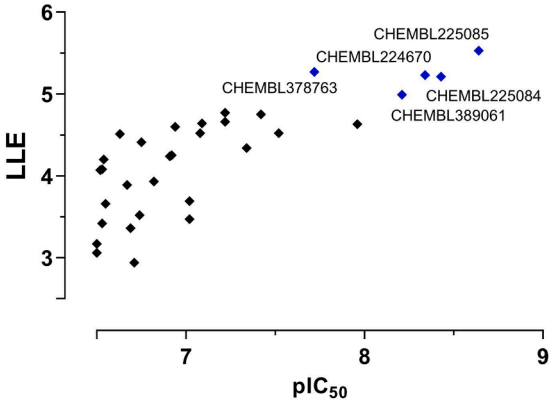


**Fig. 2.** Scatter plot depicting the activity against NEP ($pIC_{50}$) and lipophilic ligand efficiency (LLE) of selected NEP inhibitors described in the literature (ChEMBL database). LLE was calculated as the difference between $pIC_{50}$ and clogP values. Compounds CHEMBL225085 (**1a**), CHEMBL224670 (**1b**), CHEMBL225084 (**1c**) and CHEMBL378763 (**1d**) were selected for the design of codrugs bearing also an AT1 antagonist. The cyclopropylglutaramide CHEMBL389061 was not prioritized due to the more complex synthetic route to obtain the *trans*-amino cyclopropane and the concern about its chemical stability and potential to form reactive metabolites.

inhibitors. Fig. 2 shows a scatter plot containing their potency and lipophilic ligand efficiency (LLE) values. LLE is a parameter that indicates the enthalpic contribution of ligand-protein affinity as the difference between potency and the lipophilicity (LLE = $pIC_{50}$ – clogP), which is useful to guide the selection of leads with higher potential to exhibit good *in vivo* efficacy and safety (Johnson et al., 2018) . In our case, the consideration of LLE values was important to keep the size and lipophilicity of the codrugs as low as possible when incorporating potent NEPi promoities. Four NEPi described by Pryde et al. (2007) have emerged as the best options: CHEMBL225085 (**1a**), CHEMBL224670 (**1b**), CHEMBL225084 (**1c**) and CHEMBL378763 (**1d**). They display appropriate potency, physicochemical and structural features to maximize the likelihood of achieving suitable oral pharmacokinetics when combined with the AT1 promoieties in the codrugs. Although meeting the potency and LLE criteria, the cyclopropylglutaramide CHEMBL389061 was not prioritized due to the more complex synthetic route to obtain the *trans*-amino cyclopropane as well as the concern regarding its chemical stability and potential to form reactive metabolites (Pryde et al., 2007).

### 3.2. Synthesis of the novel dual-acting codrugs

We have synthesized a series of novel codrugs according to the synthetic procedures described in the Supporting Information. The functionalized glutaramides**1a, 1b, 1c** and **1d** were prepared as previously described (Maw et al., 2006; Pryde et al., 2006, 2007). The potent inhibitory activity of these compounds against NEP was confirmed in a biochemical assay ($IC_{50}$ = ~20-60 nM) and compared to sacubitrilat ($IC_{50}$ = 1.2 nM), the NEP inhibitor present in the combination LCZ696 (Table S1).

To test the concept of a codrug containing a NEPi and an AT1 antagonist, we have first explored a simple ester linker between the pharmacophores. Scheme 1 describes the synthetic route employed to generate **2a** and **2b**. The final compounds were obtained by an esterification reaction between **1a** or **1b** and **losartan**to afford **2a** and **2b**, respectively.

To further explore the linker distance and geometry between the NEP and AT1 pharmacophores, we have also synthesized compounds **3a, 3b** and **3c**. Scheme 2 illustrates the synthetic route where **E-3174** was used instead of **losartan** as starting material and reacted with 1,2-dibromoethane in the presence of potassium carbonate to afford the intermediate bromo-ethyl derivative. This intermediate was then coupled with the S-int.4 in the presence of potassium carbonate to give the benzyl protected intermediate. The benzyl group was removed by hydrogenation followed by amidation with 3-(4-Chloro-phenyl)-propylamine and deprotection of the trityl group under acidic conditions to provide **3c**.

Alternatively, **E-3174** was reacted with chloro(chlorosulfonyloxy) methane in the presence of tetrabutylammonium hydrogen sulfate and sodium bicarbonate solution to give the chloro-methyl derivative following the same synthetic steps described above to afford compound **3b** (Scheme 2). Finally, the exploration of an additional carbon atom in the linker was considered by reacting **E-3174** with 1-bromo-1-chloroethane in the presence of cesium carbonate, leading to compound **3a** as a mixture of the chiral methyl group in the linker (Scheme 2**)**.

The two remaining NEPi were incorporated in the codrugs by replacing the 3-(4-chloro-phenyl)-propylamine moiety from **3b** with an amino-thiadiazole substituent to yield the final compound **4b** or, alternatively, with a more hydrophilic substituent (2-amino-indan-2-yl)-methanol to afford the final compound **4a** (Scheme 3).

All codrugs were obtained with overall yields ranging from 30 to 47%. These variable yields obtained may be ascribed to side reactions and unavoidable losses during work up, specially by vacuum filtration, extraction, distillation steps or even during drying over sodium sulfate. Additional reaction/purification optimization may be further performed in future work to improve the overall percentage yield for the codrug candidate.

The chemical structures of the final compounds were thoroughly characterized by the combined analysis of HNMR and MS data (see Supporting Information). The HNMR spectra of compounds **2a, 2b, 3a, 3b, 3c, 4a** and **4b** and CNMR spectra of key-compound **3b** are reported in Figures S2-S8 in the Supporting Information (SI).

### 3.3. In vitro assessment of the conversion of the codrugs into the active molecules

The bioconversion of prodrugs is commonly mediated by carboxylesterases (CES), ubiquitous enzymes that hydrolyze esters, amides, carbamates and thioester prodrugs. The isoform CES1 is highly expressed in the liver, whereas the small intestine only expresses CES2. CES2 preferentially hydrolyzes substrates with a small acyl moiety due to conformational steric hindrance, while CES1 hydrolyzes a variety of bulky substrates (Wang et al., 2018), offering good opportunities for the design of prodrugs that cleave only after intestinal absorption.

The synthesized codrugs were initially incubated for 1 h with human liver and intestine S9 fractions (HLS9 and HIS9, respectively) to assess whether these systems could metabolize the ester-linked promoieties and generate the desired NEP inhibitors and AT1 antagonists. The S9 fraction system is a good *in vitro* system to model the *in vivo* clearance of prodrugs, since CES are found in both subcellular microsome and cytosolic fractions (Nishimuta et al., 2014). The codrugs **3a, 3b** and **4a** were the only ones hydrolyzed by HLS9 and generated significant concentrations of the corresponding AT1 antagonists and NEP inhibitors. The percentage of the maximal possible conversion based on the concentration of the incubated codrug (1 μM) ranged from 15 to 45% for the active molecules. Incubation with HIS9 only led to relevant amounts of the corresponding AT1 antagonist (Table 1) and not the NEPi, projecting the liver as the site of action for the conversion. Candesartan cilexetil was used as a control and showed a similar scenario. The conversion rate to candesartan was 62.5% and 13.1% when incubated with HLS9 and HIS9, respectively.

The more efficient conversion of the codrug **3b** into the AT1 antagonist (43.1%) and NEP inhibitor (30.3%) in HLS9 when compared to the other codrugs and less efficiently in HIS9 has prompted us to further investigate the *in vitro* properties of **3b** before its *in vivo* assessment. Table 2 illustrates the stability of **3b** in aqueous buffers and simulated biological fluids at different pHs as well as its solubility. **3b** was very stable in SGF and in aqueous buffers at pH 1.1, 6.5 and 7.4, and showed good stability in SIF. **3b** also exhibited adequate solubility at pH 7.4. We have not assessed the cell permeability of codrug **3b** because it would be little informative: (i) the *in vitro* permeability models do not show good correlation with oral absorption data for beyond rule-of-5 compounds (Doak et al., 2014) and (ii) despite demonstrating good oral absorption, candesartan cilexetil (our control) displayed very poor permeability in a preliminary MDCK permeability (Irvine et al., 1999) test (Table S2).

Before performing *in vivo* studies (PK and efficacy) in rats, we have also conducted an interspecies comparison of **3b** metabolism using liver S9, intestine S9 and plasma from rat and human (Fig. 3). **3b** was as efficiently converted into the active **E-3174** and **1a** molecules in rat liver S9 as it was in human. Similar to human, rat intestine S9 only generated **E-3174**, to a lower degree than in the liver, and did not generate **1a**. While human and rat seem to be aligned in terms of S9 data, the situation was very different between the two species in plasma. **3b** was very stable in human plasma and did not generate **E-3174** and **1a** appreciably, while it was extensively cleaved in rat plasma into the desired molecules. Candesartan cilexetil was also used as a control in plasma and, again, a similar scenario to **3b** emerged. Candesartan cilexetil was poorly converted into candesartan in human plasma; 69.7% of candesartan cilexetil still remained after 120 min (half-life = 15.9 ± 0.3 h) and only 3.9% of candesartan was generated. Taken together, the *in vitro* data suggests that codrug **3b**, after dissolution, should demonstrate good stability in different gastrointestinal compartments upon oral administration to humans and rats, partially cleaved in the intestine by CES2

**Table 1**
Conversion of the codrugs at 1 μM into the corresponding AT1 antagonist and NEP inhibitor in human liver and intestine S9 fractions.

| Codrug | Stability in human liver S9 | | | Stability in human intestine S9 | | |
|---|---|---|---|---|---|---|
| | $t_{1/2}$ (min) | Conversion to NEPi (%, 1h) | Conversion to AT1 antagonist (%, 1h) | $t_{1/2}$ (min) | Conversion to NEPi (%, 1h) | Conversion to AT1 antagonist (%, 1h) |
| **2a** | 7.5 | 0.4 | 15.3 | 23.5 | 0.3 | 8.1 |
| **2b** | 6.2 | 0.4 | 13.2 | 12.7 | 0.4 | 8.1 |
| **3a** | 5.2 | 15.6 | 43.4 | 13.1 | 0.5 | 21.5 |
| **3b** | 2.1 | 30.3 | 43.1 | 11.6 | 2.4 | 18.4 |
| **3c** | 2.6 | 1.2 | 0.4 | 5.5 | 0.2 | 0.3 |
| **4a** | 2.6 | 18.1 | 43.8 | 8.4 | 0.1 | 24.4 |
| **4b** | ND | ND | ND | ND | ND | ND |
| **Candesartan cilexetil** | 0.7 | - | 62.5 | 73.7 | - | 13.1 |

$t_{1/2}$ - compound disappearance half-life. NEPi – Neprilysin inhibitor. ARB – Angiotensin II receptor blockers or AT1 antagonist. ND – Not determined due to instability in the assay buffer. The codrugs were incubated with human liver and intestine S9 fraction for 60 min and their conversion to the active molecules were assessed. The active molecules were: (i) 1a and E-3174 for 3a, 3b and 3c, (ii) 1a and losartan for 2a, (iii) 1b and losartan for 2b, (iv) 1c and E-3174 for 4a and (v) candesartan for candesartan cilexetil.

**Table 2**
*In vitro* stability and solubility properties of codrug **3b**.

| Assay | pH | Parameter | |
|---|---|---|---|
| Aqueous buffer stability | 1.1 | $t_{1/2}$ (hour) | >24 h |
| | 6.5 | | >24 h |
| | 7.4 | | >24 h |
| Simulated gastric fluid | 1.2 | | >24 h |
| Simulated intestinal fluid | 6.8 | | 3.6 h (0.4) |
| Kinetic solubility | 7.4 | Solubility (μM) | 3.8 μM (0.2) |

Data is shown as mean (S.D.), n = 2. $t_{1/2}$ – compound disappearance half-life.

generating mainly the AT1 antagonist **E-3174** and then more efficiently cleaved by CES1 in the liver into the two active molecules, **E-3174** and **1a**. In rat plasma, **3b** is further cleaved into the active molecules very effectively, while the same does not occur in human plasma, projecting a very good oral PK in rats, but less clear in humans.

### *3.4. Oral bioavailability of the AT1 antagonist E-3174 and the NEP inhibitor 1a upon administration of codrug 3b compared to direct administration of losartan, E-3174 and 1a in different rat strains*

We have then decided to assess the *in vivo* PK behavior of codrug **3b** after oral (10 mg/kg) and intravenous (1 mg/kg) administration to Sprague Dawley (SD) rats (Table 3 and Table S3, respectively). The PK parameters of **3b** and its active promoieties **E-3174** and **1a** were compared to those of **losartan, E-3174** and **1a** administered directly to SD rats. As projected by the *in vitro* data, the oral administration of **3b** resulted in good bioavailability of both the AT1 antagonist **E-3174** and the NEP inhibitor **1a**. These compounds were identified in plasma samples up to 24 hours after oral dosing, as shown in Fig. 4. Oral administration of **E-3174** directly to SD rats, as expected, resulted in a very poor oral bioavailability (F = 3.5%) due to the presence of two ionizable acidic groups, one carboxylic acid and one tetrazole group. In contrast, the oral administration of **3b**yielded a much higher bioavailability of **E-3174** (F = 14.6%) than the direct oral administration of **E-3174** itself and even oral administration of **losartan**, which yielded an oral bioavailability of 6.3% for **E-3174**. If we account for molar differences between the administered oral doses in mg/kg, the AUC value of **E-3174** upon oral administration of **3b** was about twice and four times as high the AUC values of **E-3174** upon oral administration of **losartan** and **E-3174**, respectively (Table 3). The animals orally dosed with **3b** also had appreciable bioavailability for the NEP inhibitor **1a** (F = 10.4%), although the direct administration of **1a** resulted in a much higher oral bioavailability (F= 67.9%), as **1a** has drug-like physicochemical properties.

The *in vivo* PK of codrug **3b** was further evaluated in the spontaneous hypertensive rat (SHR), as this species was the one used in the hypertensive model. **3b** was dosed at 10, 30 and 60 mg/kg p.o. – possible doses in the efficacy model. The plasma exposure of the active promoiety **E-3174** was compared to those of animals dosed **losartan** and **E-3174** directly at 10 mg/kg p.o. and the plasma exposure of the active promoiety **1a** was compared to that of animals dosed **1a** directly at 10 mg/kg p.o. (Table 4). Compounds **E-3174** and **1a** were also dosed intravenously at 1 mg/kg to afford the determination of their oral bioavailability (Table S4). The oral administration of **3b** has yielded a dose-dependent and proportional increase in the plasma levels of **E-3174** and **1a** in SHR rats. The bioavailability of **E-3174** upon oral administration of **3b** at 10, 30 and 60 mg/kg was 40.9, 33.7 and 49.7%, respectively, much higher than the values obtained after oral administration of **losartan** and **E-3174** itself (F = 10.3 and 9.5%, respectively). The plasma exposure of **1a** following oral administration of **3b** was also very good, with F values ranging from 9.2 to 18.4%. The AUC values for **1a** ranged from 1,824 to 15,410 h*ng/mL. Specifically, the AUC value for **1a** after oral administration of **3b** at 60 mg/kg (or 71.02 μmol/kg) delivered similar AUC values of **1a** compared to its direct oral administration at 10 mg/kg (or 25.26 μmol/kg). Fig. 5 shows that **3b** was rapidly converted to the active molecules in plasma and that both **E-3174** and **1a** displayed good plasma levels over 24 hours after 10, 30 and 60 mg/kg of **3b**p.o.

### *3.5. Antihypertensive effects of codrug 3b compared to losartan alone and combined with the NEP inhibitor 1a in the SHR model*

The acute antihypertensive effects of codrug **3b** at 10, 30 and 60 mg/kg p.o., the AT1 antagonist **losartan** (15 mg/kg p.o.) alone and combined with the NEP inhibitor **1a** (15 mg/kg p.o. of **losartan** + 14 mg/kg p.o. of **1a**) were evaluated in the SHR model over 24 hours (Fig. 6). The systolic blood pressure (SBP), diastolic blood pressure (DBP) and heart rate (HR) were measured at pre-dose, 1, 2, 4, 8 and 24 h after dosing, and the mean arterial pressure (MAP) was determined as DBP + 1/3 (SBP – DBP) at each time point. We have also calculated the variation (Δ) of these parameters over time in comparison to the pre-dose values, and then estimated the area under the curve (AUC) for each parameter and group. Statistically significant differences in blood pressure were identified by two-way (over time) or one-way (AUC) ANOVA followed by the Holm-Sidak post-hoc test.

The two-way ANOVA has shown statistically significant differences between the groups for the parameters ΔSBP ($F(5,42) = 5.15$, $p<0.01$), ΔDBP ($F(5,42) = 4.32$, $p<0.01$) and ΔMAP ($F(5,42) = 4.39$, $p<0.01$). All treated groups had statistically significantly lower ΔSBP (Fig. 6A), ΔDBP (Fig. 6C) and ΔMAP (Fig. 6E) at 4 h and 8 h ($p<0.05$) in comparison to vehicle. Interestingly, only the groups treated with codrug **3b** at 30 and 60 mg/kg p.o. or with the combination **losartan** + **1a** had sustained lowering effects in ΔSBP and ΔMAP at the 24 h timepoint ($p<0.05$). On

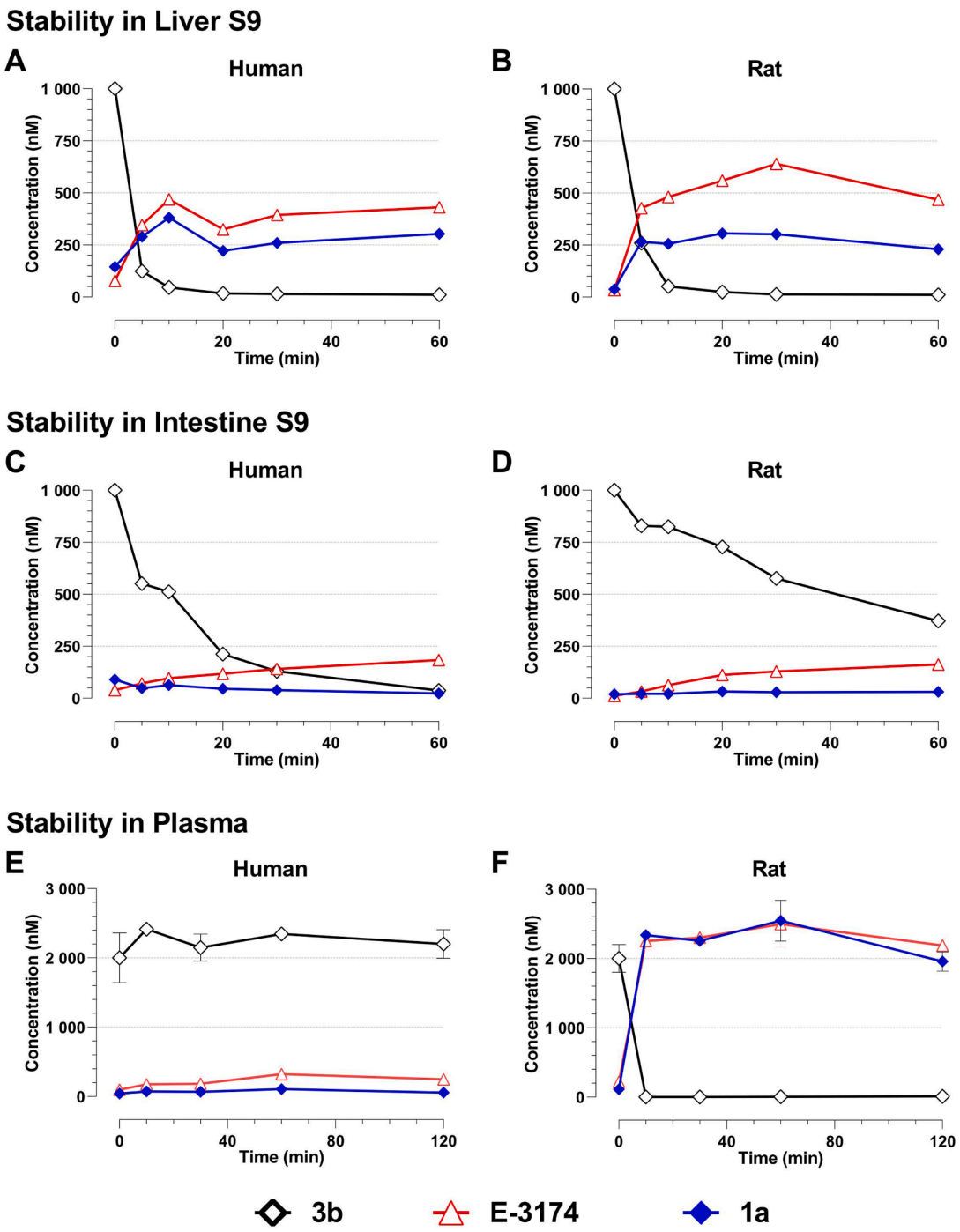


**Fig. 3.** *In vitro* metabolic stability of codrug 3b and its conversion into the active molecules **E-3174** and **1a** in liver S9, intestine S9 and plasma of humans and SD rats.

the other hand, significantly reduced ΔDBP values were only seen for the groups treated with **3b** at 30 and 60 mg/kg at 24 h ($p<0.01$). No statistically significant differences in ΔHR were observed (Fig. 6G).

The results from the one-way ANOVA using the AUC data were also in line with those from the two-way ANOVA. There were significant differences in ΔSBP AUC (Fig. 6B, $F(5,42) = 19.94$, $p<0.0001$), ΔDBP AUC (Fig. 6D, $F(5,42) = 15.56$, $p<0.0001$) and ΔMAP AUC (Fig. 6F, $F(5,42) = 18.15$, $p<0.0001$) between the groups. The pairwise comparisons against vehicle for the ΔSBP, ΔDBP and ΔMAP AUC parameters were all statistically significant ($p<0.01$), whereas the AUC comparisons against **losartan**-treated animals showed that only **3b** exhibited lower ΔSBP (30 and 60 mg/kg p.o., $p<0.01$), ΔDBP (60 mg/kg p.o., $p<0.05$) and ΔMAP (30 and 60 mg/kg p.o., $p<0.05$) AUC values. In addition, the comparisons against the group treated with the combination **losartan** + **1a** further evidenced the significant BP-lowering effects of **3b** when analyzing the ΔSBP (30 and 60 mg/kg p.o., $p<0.05$) and ΔDBP (60 mg/kg p.o., $p<0.05$) AUC parameters. It is important to note that the 30 mg/kg dose of **3b** is mole-by-mole equivalent to the combination of 15 mg/kg of **losartan** + 14 mg/kg of **1a**.

## 4. Discussion

We have explored here the concept of codrugs carrying an AT1 antagonist and a NEP inhibitor to develop novel, more efficacious, and safer antihypertensive agents. Analyzing the chemical space of AT1 antagonists and NEP inhibitors, there would be several potential

**Table 3**
*In vivo* PK of codrug **3b, E-3174, losartan**, and **1a** in SD rats.

| Compound | Analyte | p.o. | | | i.v. | | |
|---|---|---|---|---|---|---|---|
| | | Dose (mg/kg [μmol/kg]) | F (%) | $C_{max}$(ng/mL) | $AUC_{0\text{-}inf}$ (h*ng/mL) | Dose (mg/kg [μmol/kg]) | $AUC_{0\text{-}inf}$ (h*ng/mL) |
| **E-3174** | **E-3174** | 10 [22.89] | 3.5 (0.6) | 1,112 (179) | 5,708 (1,027) | 1 [2.29] | 16,419 (2,151) |
| **1a** | **1a** | 10 [25.26] | 67.9 (11.2) | 12,967 (808) | 37,182 (6,106) | 1 [2.53] | 5,472 (3,377) |
| **3b** | **3b** | 10 [11.84] | 0.8 (0.6) | 22.1 (7.4) | 16.5 (12.2) | 1 [1.18] | 214.8 (87.0) |
| | **E-3174** | - | 14.6 (2.0) | 3,957 (895) | 12,431 (1,696) | - | - |
| | **1a** | - | 10.4 (4.5) | 1,187 (281) | 2,655 (1,142) | - | - |
| **Losartan** | **Losartan** | 10 [23.65] | 29.3 (7.6) | 1,323 (654) | 4,714 (1,216) | 1 [2.36] | 1,608 (220b) |
| | **E-3174** | - | 6.3 (0.6) | 1,387 (195) | 10,661 (955) | - | - |

The compounds were administered to male SD rats at 1 mg/kg i.v. and 10 mg/kg p.o., n=3 animals per group. Data is shown as mean (S.D.). F - Bioavailability. $C_{max}$ – maximum plasma concentration. $AUC_{0\text{-}inf}$ - area under the curve from time 0 extrapolated to infinite time. The active molecules were also quantified after dosing with the parent codrug 3b (E-3174 and 1a) or losartan (E-3174).

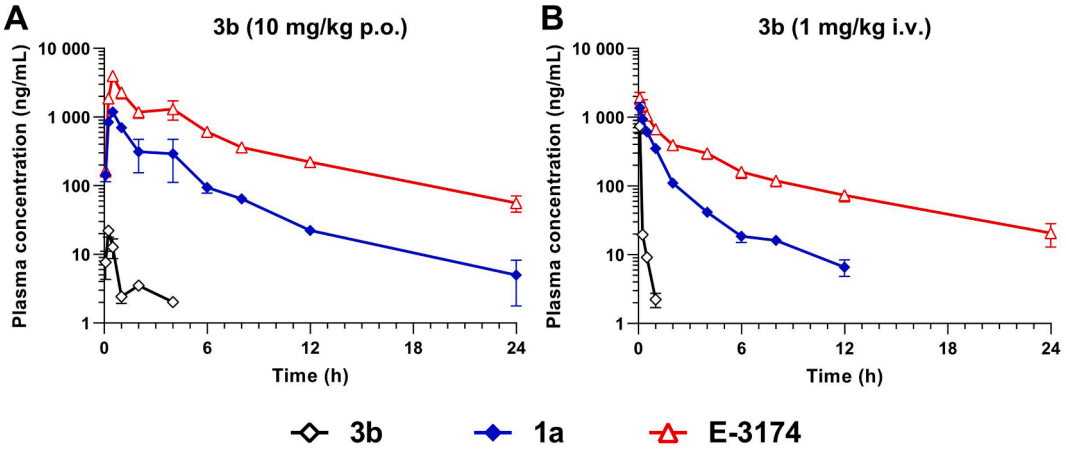


**Fig. 4.** Plasma concentrations of codrug **3b** and its conversion to the active molecules **E-3174** and **1a** after oral and intravenous administration to SD rats. Codrug **3b** was administered to male SD rats at 1 mg/kg i.v. and 10 mg/kg p.o., n=3 animals per group. Data is shown as mean ± S.E.M. The active molecules (**E-3174** and **1a**) were also quantified after the administration of the parent codrug **3b**.

**Table 4**
*In vivo* pharmacokinetics of codrug **3b, E-3174, losartan**, and**1a** in SHR rats.

| Compound | Analyte | | | p.o. | | i.v. | |
|---|---|---|---|---|---|---|---|
| | | Dose (mg/kg [μmol/kg]) | F (%) | $C_{max}$(ng/mL) | $AUC_{0\text{-}inf}$ (h*ng/mL) | Dose (mg/kg [μmol/kg]) | $AUC_{0\text{-}inf}$ (h*ng/mL) |
| **E-3174** | **E-3174** | 10 [22.89] | 9.5 (3.4) | 1,084 (317) | 10,862 (3,821) | 1 [2.29] | 11,510 (1,067) |
| **1a** | **1a** | 10 [25.26] | 42.8 (4.4) | 7,963 (956) | 12,768 (1,311) | 1 [2.53] | 2,985 (543) |
| **3b** | **3b** | 10 [11.84] | ND | 34.3 (37.4) | 100.9 (84.0) | - | - |
| | **E-3174** | - | 40.9 (19.8) | 2,873 (697) | 24,104 (11,657) | - | - |
| | **1a** | - | 13.0 (5.3) | 654.7 (444.6) | 1,824 (748) | - | - |
| **3b** | **3b** | 30 [35.51] | ND | 180.0 (33.0) | 216.7 (52.3) | - | - |
| | **E-3174** | - | 33.7 (5.9) | 11,007 (2,506) | 59,548 (10,348) | - | - |
| | **1a** | - | 9.2 (1.3) | 1,096 (220) | 3,882 (535) | - | - |
| **3b** | **3b** | 60 [71.02] | ND | 374.3 (113.1) | 784 (184) | - | - |
| | **E-3174** | - | 49.7 (6.9) | 25,967 (1,550) | 175,694 (24,550) | - | - |
| | **1a** | - | 18.4 (3.3) | 4,577 (1,061) | 15,410 (2,776) | - | - |
| **Losartan** | **Losartan** | 10 [23.65] | ND | 1,507 (330) | 7,734 (2,053) | - | - |
| | **E-3174** | - | 10.3 (2.0) | 1,313 (60.3) | 11,747 (2,279) | - | - |

The active molecules E-3174 and 1a were administered to male SHR rats at 1 mg/kg i.v. Losartan, E-3174, and 1a were administered at 10 mg/kg p.o.. Codrug 3b was administered at 10, 30 or 60 mg/kg p.o.. n=3 animals was used per group. Data is shown as mean (S.D.). ND – Not determined. F - Oral bioavailability. $C_{max}$ – maximum plasma concentration. $AUC_{0\text{-}inf}$ - area under the curve from time 0 extrapolated to infinite time. The active molecules were also quantified after the administration of the parent codrug 3b (E-3174 and 1a) and Losartan (E-3174).

advantages of administering a codrug instead of directly dosing a combination of parent compounds, their co-crystals or prodrug versions of each compound, such as improved solubility, enhanced permeability, prolonged half-life, better safety profile, and synergistic effects due to matched pharmacokinetics and delivery at the sites of action (Aljuffali et al., 2016). We have then designed, synthesized, and evaluated few possibilities to select a tool codrug, a minimum viable compound, to demonstrate the feasibility of the concept.

The codrugs were tested *in vitro* using HLS9 and HIS9 to assess their potential to be hydrolyzed into the AT1 and NEP pharmacophores. Compound **3b** emerged as the most effectively hydrolyzed compound from this screening and the results pointed to the liver - the desirable location - as the site of metabolism. The conversion of **3b** into the active molecules was further evaluated in rat liver and intestine S9 fractions. A good alignment between species emerged; **3b** was rapidly and effectively cleaved into the desired molecules in the presence of rat liver S9

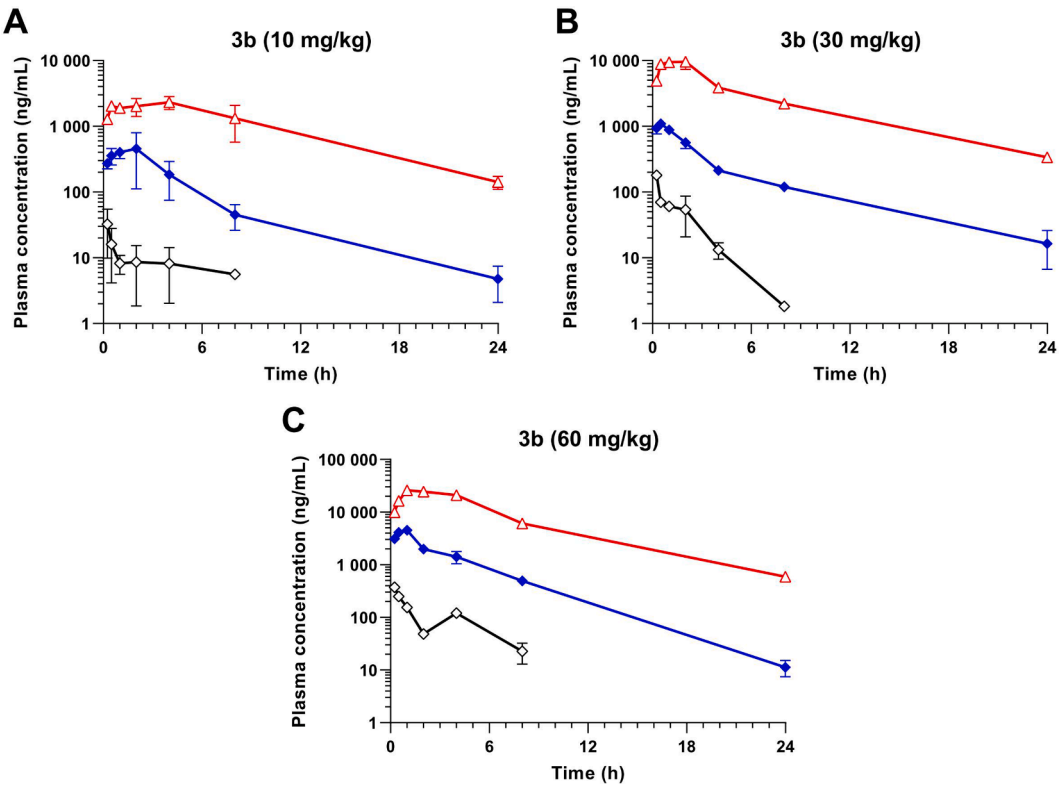


**Fig. 5.** Plasma concentrations of codrug **3b** and its conversion to the active molecules **E-3174** and **1a** after oral administration to SHR rats. Codrug **3b** was administered to male SHR rats at 10, 30 or 60 mg/kg p.o., n=3 animals per group. Data is shown as mean ± S.E.M. The active molecules (**E-3174** and **1a**) were also quantified after the administration of the parent codrug **3b**.

and not effectively in rat intestine S9, generating only reduced concentrations of **E-3174**. In plasma, however, the scenario was quite different between human and rat. **3b** was quite stable in human plasma, but rapidly metabolized in rat plasma to produce **E-3174** and **1a**. Nishimuta et al. (2014) have found similar interspecies differences between human and rat for other prodrugs. For example, candesartan cilexetil was efficiently converted into candesartan in hepatocytes and liver S9 fractions from both species, whereas a high stability for candesartan cilexetil in human plasma was opposed to an evident hydrolysis in rat plasma after a 60-minute incubation. Recent studies have also demonstrated the same interspecies differences in the plasma metabolism of other prodrugs due to variations in the expression profiles of esterases. While CES1 and CES2 are all expressed abundantly in human, dog, and rat liver and intestine, respectively, CES expression in plasma differs quite significantly between species; rat plasma displays high CES expression, while human and dog plasma do not have detectable CES activity (Fu et al., 2016; Williams et al., 2011). Indeed, CES are the major enzymes involved in the hydrolysis of ester prodrugs in rats, while other plasma esterases may play a role in dogs and humans (Bhuket et al., 2019).

The additional *in vitro* data generated suggests that codrug **3b**, after dissolution, should demonstrate good chemical stability upon oral administration, partially cleaved in the intestine by CES2 generating mainly the AT1 antagonist **E-3174** and then more efficiently by CES1 in the liver generating **E-3174** and **1a**. In rat plasma, **3b** is further cleaved into the active molecules but the same does not occur in human plasma, projecting at least a very good oral PK in rats. In fact, the oral dosing of **3b** in rats has resulted in high plasma levels of the compounds of interest over 24 hours. The low plasma exposure of **E-3174** after its direct oral dosing, compared to a very high plasma exposure for **E-3174** upon **3b** administration, indicates that the formation of this AT1 antagonist indeed occurs mostly in the liver after intestinal absorption in rodents. The intravenous administration of **3b** also delivers high plasma levels of the active compounds, further corroborating the liver as the organ where the conversion takes place. The HLS9 and HIS9 data for **3b** projects a similar scenario in human, being the main difference between human and rat the continuous conversion in plasma for the latter. Taken together, the *in vitro* and *in vivo PK* data for **3b** supported it as a candidate for a tool codrug in animal efficacy studies.

We have then evaluated the antihypertensive effects of codrug **3b** in comparison to those of **losartan** alone or combined with the NEP inhibitor **1a** in SHR rats, a normal renin, sodium-independent hypertension animal model. This model has pathological alterations that are also present in human hypertension such as increased vascular resistance and increased BP response to Ang II. Consequently, it has been broadly applied to assess the pharmacological effects of novel drugs (Pinto et al., 1998). Indeed, the hemodynamic changes seen in the SHR model respond to many drug classes clinically approved for treating hypertension, including ARBs (Lerman et al., 2019). The administration of **3b**at 30 and 60 mg/kg p.o. in SHR rats led to a statistically significant reduction in BP-related parameters, such as SBP, DBP and MAP, that were significantly lower than the observed in rodents treated either with **losartan** alone or combined with **1a**. Though very important from the synergy point of view**,** it should be mentioned that the superior results obtained with **3b** versus **losartan** are not necessarily associated with the additional delivery of the NEP inhibitor **1a** only. The PK comparisons in Table 4 suggest that the much better PK profile for **E-3174** upon **3b** administration should play an important role too. This should also likely explain the superior results obtained with the 30 mg/kg dose of **3b** versus its mole-by-mole equivalent comparator, the combination of **losartan** (15 mg/kg p.o.) and **1a** (14 mg/kg p.o.). For instance, rats dosed with **3b** at 30 and 60 mg/kg p.o. exhibited $C_{max}$ values for **E-3174** that were supra-proportional by many multiples the one expected for **E-3174** in **losartan**- and **losartan**+**1a**- treated animals. Moreover, the acute oral administration of the codrug **3b**, but not of **losartan**, induced a sustained reduction in BP up to 24 hours post-dose, in agreement with

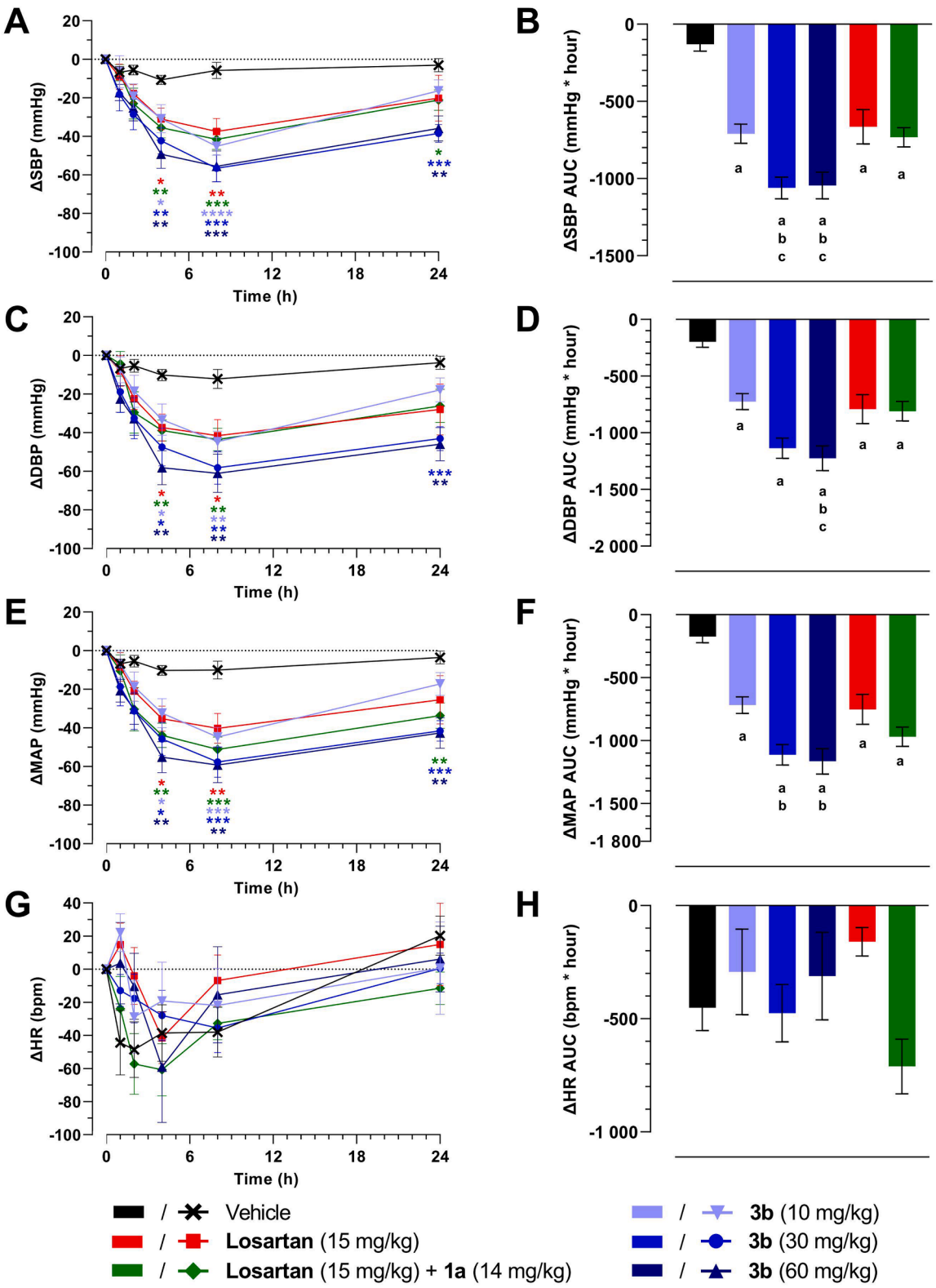


**Fig. 6.** Acute oral antihypertensive effects of **3b, losartan**and **1a** in SHR rats.(A-B) Systolic, (C-D) diastolic and (E-F) mean arterial blood pressure, and (G-H) heart rate were assessed following acute oral administration of **3b** (10, 30 and 60 mg/kg), **losartan**(15 mg/kg), **losartan** + **1a** (15 and 14 mg/kg, respectively) or vehicle to male SHR rats. Data is shown as the mean ± S.E.M. of the SBP, DBP, MAP and HR reduction over time and was analyzed by two-way ANOVA followed by the Holm-Sidak post-hoc test. Statistically significant differences *vs* vehicle are denoted by * ($p<0.05$), ** ($p<0.01$), *** ($p<0.001$) and **** ($p<0 .0001$). AUC data was analyzed by one-way ANOVA and the Holm-Sidak test. Statistically significant differences ($p<0.05$) are denoted by [a]*vs* vehicle, [b]vs **losartan**and [c]*vs* **losartan** + **1a** groups.

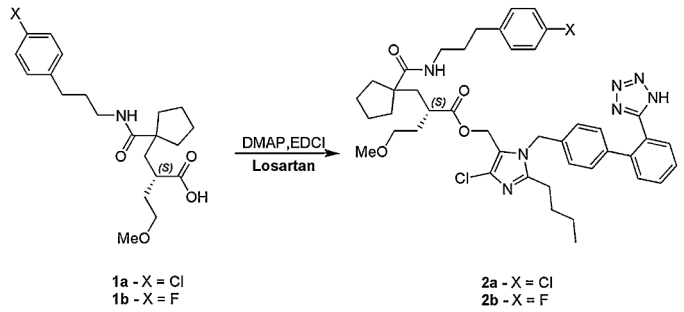


**Scheme 1.** Synthesis of compounds **2a** and **2b**.

the detectable levels of both AT1 and NEP inhibitors over the 24 hours. This PK/PD profile supports the potential use of a codrug like **3b** as a once-daily therapy, representing an important advantage over LCZ696, which requires BID dosing for appropriate 24-hour inhibition of both targets. The twice daily posology of LCZ696 may limit its long-term clinical impact in heart failure patients due to potential decrease in treatment adherence over the years (Weeda et al., 2016).

Codrug **3b** combines the AT1 antagonist **E-3174, losartan**'s more active metabolite, and the lipophilic efficient NEP inhibitor **1a**. When compared to **losartan**, the administration of codrug **3b** offers specific benefits, such as bypassing the CYP2C9-mediated conversion of **losartan** to **E-3174**, mitigating CYP2C9 polymorphism, reducing the risk of drug-drug interactions with common antihypertensive agents that are CYP2C9 substrates or inhibitors, and preventing the potential formation of **losartan**-derived reactive metabolites that could lead to idiosyncratic drug-induced liver injury. It is important to highlight that codrug **3b** offers benefits not only over **losartan** but also over **E-3174**, as this metabolite would be poorly absorbed if dosed directly. Finally, codrug **3b** is able to do all that, while providing meaningful plasma concentrations of the NEP inhibitor **1a** for optimal synergy with the AT1 antagonist. In summary, we demonstrate here that the concept of codrugs carrying an AT1 antagonist and a NEP inhibitor is a viable option over standalone AT1 blocking therapies and their fixed-dose combinations with NEP inhibitors; compound **3b**, the tool codrug discovered in this work, represents a stepping stone in the pathway to obtain an once-daily, dual-acting codrug clinical candidate for the treatment of hypertension and heart failure.

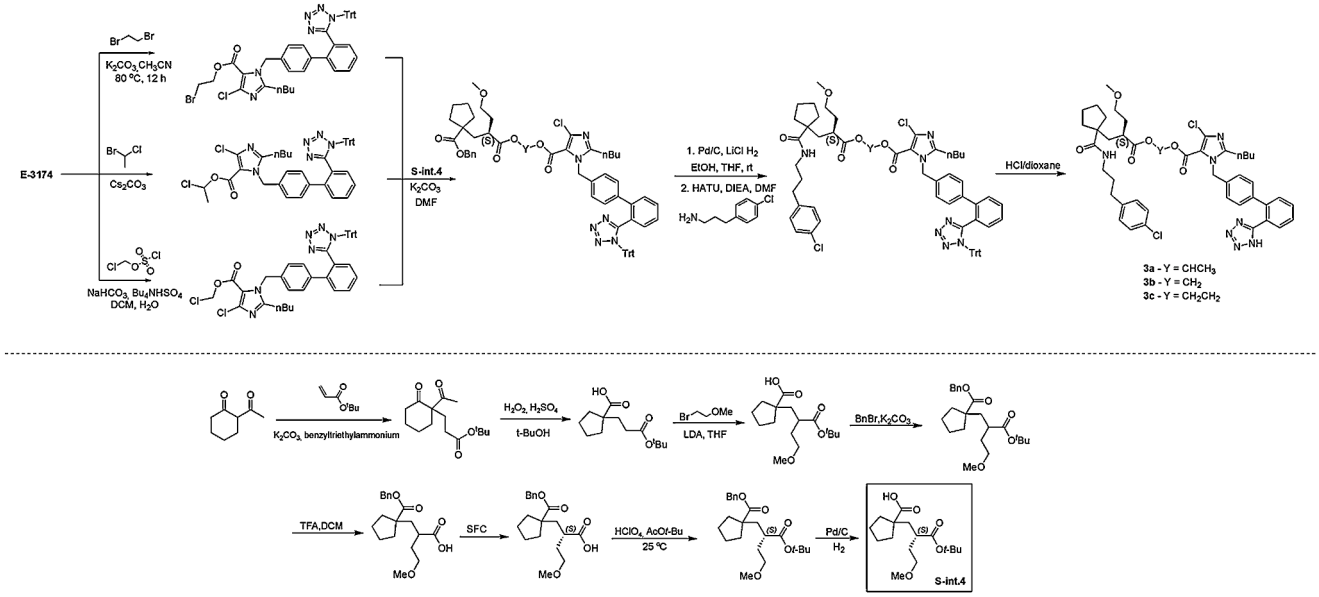


**Scheme 2.** Synthesis of compounds **3a, 3b** and **3c**.

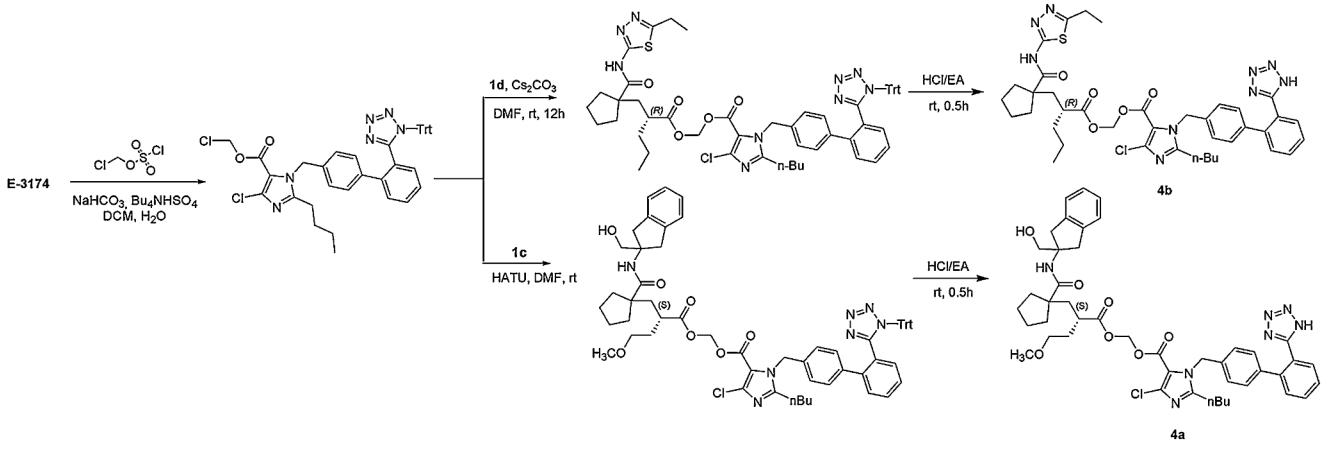


**Scheme 3.** Synthesis of compounds **4a** and **4b**.

## Authors Contributions

AM and EEI conducted the synthesis activities to obtain the compounds. AM, HA, MF, EEI and CRWG designed the compounds and the biological experiments, analyzed the results and drafted the manuscript. All authors reviewed the final version of the manuscript.

## Funding

This research was financed by Aché Laboratórios Farmacêuticos, wherein AM, HA, MF, EEI and CRWG were employed during the execution of this work.

## Declaration of Competing Interest

None.

## Acknowledgements

We appreciate the insights provided by Dr. Ronaldo Adriano Timm about solid-state engineering approaches and their impact on the discovery and development of co-crystals and codrugs.

## Supplementary materials

Supplementary material associated with this article can be found, in the online version, at doi:10.1016/j.ejps.2021.105731.

## References

Aljuffali, I.A., Lin, C.F., Chen, C.H., Fang, J.Y., 2016. The codrug approach for facilitating drug delivery and bioactivity. Expert Opin. Drug Deliv. 13, 1311–1325. https://doi.org/10.1080/17425247.2016.1187598.

Barreras, A., Gurk-Turner, C., 2003. Angiotensin II receptor blockers. Proceedings (Baylor University. Medical Center) 16, 123–126. https://doi.org/10.1080/08998280.2003.11927893.

Bausell, R.B., Li, Y.F., 2002. Power analysis for experimental research: A practical guide for the biological, medical, and social sciences. Cambridge University Press, New York, NY.

Bavishi, C., Messerli, F.H., Kadosh, B., Ruilope, L.M., Kario, K., 2015. Role of neprilysin inhibitor combinations in hypertension: insights from hypertension and heart failure trials. Eur. Heart J. 36, 1967–1973. https://doi.org/10.1093/eurheartj/ehv142.

Braunwald, E., 2015. The path to an angiotensin receptor antagonist-neprilysin inhibitor in the treatment of heart failure. J. Am. Coll. Cardiol. 65, 1029–1041. https://doi.org/10.1016/j.jacc.2015.01.033.

Christen, Y., Waeber, B., Nussberger, J., Porchet, M., Borland, R.M., Lee, R.J., Maggon, K., Shum, L., Timmermans, P.B., Brunner, H.R., 1991. Oral administration of DuP 753, a specific angiotensin II receptor antagonist, to normal male volunteers. Inhibition of pressor response to exogenous angiotensin I and II. Circulation 83, 1333–1342. https://doi.org/10.1161/01.cir.83.4.1333.

Daly, A.K., Rettie, A.E., Fowler, D.M., Miners, J.O., 2017. Pharmacogenomics of CYP2C9: Functional and Clinical Considerations. J. Personal. Med. 8, 1. https://doi.org/10.3390/jpm8010001.

Doak, B.C., Over, B., Giordanetto, F., Kihlberg, J., 2014. Oral druggable space beyond the rule of 5: insights from drugs and clinical candidates. Chem. Biol. 21 (9), 1115–1142. https://doi.org/10.1016/j.chembiol.2014.08.013.

Feng, L., Karpinski, P.H., Sutton, P., Liu, Y., Hook, D.F., Hu, B., et al., 2012. LCZ696: A dual-acting sodium supramolecular complex. Tetrahedron Lett. 53, 275–276. https://doi.org/10.1016/j.tetlet.2011.11.029.

Food and Drug Administration, 2018. Regulatory Classification of Pharmaceutical Co-Crystals Guidance for Industry. Center for Drug Evaluation and Research (CDER).

Fu, J., Pacyniak, E., Leed, M., Sadgrove, M.P., Marson, L., Jay, M., 2016. Interspecies Differences in the Metabolism of a MultiesterProdrug byCarboxylesterases. J. Pharma. Sci. 105, 989–995. https://doi.org/10.1002/jps.24632.

Gaudet, E., Blanc, J., Elghozi, J.L., 1995. Effects of losartan on short-term variability of blood pressure in SHR and WKY rats. Fundament. Clin. Pharmacol. 9 (1), 30–36.

Guo, H., Zhuang, X., Qian, K., Sun, L., Wang, X., Li, H., Lee, K., Xie, L., 2012. Prodrug design, synthesis and pharmacokinetic evaluation of (3′ R, 4′ R)-3-hydroxymethyl-4-methyl-3′,4′-di-O-(S)-camphanoyl-(+)-cis-khellactone. Acta Pharm. Sin. B 2, 213–219. https://doi.org/10.1016/j.apsb.2012.02.008.

Hubers, S.A., Brown, N.J., 2016. Combined Angiotensin Receptor Antagonism and Neprilysin Inhibition. Circulation 133, 1115–1124. https://doi.org/10.1161/CIRCULATIONAHA.115.018622.

Irvine, J.D., Takahashi, L., Lockhart, K., Cheong, J., Tolan, J.W., Selick, H.E., Grove, J.R., 1999. MDCK (Madin-Darby canine kidney) cells: A tool for membrane permeability screening. J. Pharma. Sci. 88 (1), 28–33. https://doi.org/10.1021/js9803205.

Iwamura, A., Fukami, T., Hosomi, H., Nakajima, M., &Yokoi, T., 2011. CYP2C9-mediated metabolic activation of losartan detected by a highly sensitive cell-based screening assay. Drug metabolism and disposition: the biological fate of chemicals. 39, 838–846. doi: 10.1124/dmd.110.037259.

Johnson, G.D., Ahn, K., 2000. Development of an internally quenched fluorescent substrate selective for endothelin-converting enzyme-1. Anal. Biochem. 286, 112–118. https://doi.org/10.1006/abio.2000.4772.

Johnson, T.W., Gallego, R.A., Edwards, M.P., 2018. Lipophilic Efficiency as an Important Metric in Drug Design. J. Med. Chem. 61, 6401–6420. https://doi.org/10.1021/acs.jmedchem.8b00077.

Joy, M.S., Dornbrook-Lavender, K., Blaisdell, J., Hilliard, T., Boyette, T., Hu, Y., Hogan, S.L., Candiani, C., Falk, R.J., Goldstein, J.A., 2009. CYP2C9 genotype and pharmacodynamic responses to losartan in patients with primary and secondary kidney diseases. Eur. J. Clin. Pharmacol. 65, 947–953. https://doi.org/10.1007/s00228-009-0707-7.

Kavanagh, O.N., Croker, D.M., Walker, G.M., Zaworotko, M.J., 2019. Pharmaceutical cocrystals: from serendipity to design to application. Drug Discov. Today 24, 796–804. https://doi.org/10.1016/j.drudis.2018.11.023.

Lerman, L.O., Kurtz, T.W., Touyz, R.M., Ellison, D.H., Chade, A.R., Crowley, S.D., Mattson, D.L., Mullins, J.J., Osborn, J., Eirin, A., Reckelhoff, J.F., Iadecola, C., Coffman, T.M., 2019. Animal models of hypertension: a scientific statement from the. American Heart Association. Hypertension. 73, e87–e120. https://doi.org/10.1161/HYP.0000000000000090.

Lipinski, C. A., Lombardo, F., Dominy, B. W., &Feeney, P. J., 2001. Experimental and computational approaches to estimate solubility and permeability in drug discovery and development settings. Advanced drug delivery reviews. 46, 3–26. doi: 10.1016/s0169-409x(00)00129-0.

Mannhold, R., Poda, G.I., Ostermann, C., Tetko, I.V., 2009. Calculation of molecular lipophilicity: State-of-the-art and comparison of log P methods on more than 96,000 compounds. J. Pharm. Sci. 98 (3), 861–893. https://doi.org/10.1002/jps.21494.

Maslov, M.Y., Foianini, S, Mayer, D., Orlov, M.V., Lovich, M.A., 2019. Synergy between sacubitril and valsartan leads to hemodynamic, antifibrotic, and exercise tolerance benefits in rats with preexisting heart failure. Am. J. Physiol. Heart Circ. Physiol. 316, H289–H297.

Maw, G.N., Stobie, A., Planken, S., Pryde, D.C., Sanderson, V., Platts, M.Y., Corless, M., Stacey, P., Wayman, C., Van Der Graaf, P., Kohl, C., Coggon, S., Beaumont, K., 2006. The discovery of small molecule inhibitors of neutral endopeptidase. Structure-activity studies on functionalized glutaramides. Chem. Biol. Drug Des. 67, 74–77. https://doi.org/10.1152/ajpheart.00579.

McMurray, J.J., et al., 2014. Angiotensin-neprilysin inhibition versus enalapril in heart failure. N Engl J Med. 2014 Sep 11;371(11):993-1004. doi: 10.1056/NEJMoa1409077. N. Engl. J. Med. 371 (11), 993–10004. https://doi.org/10.1056/NEJMoa1409077.

Miura, S., Karnik, S.S., Saku, K., 2011. Review: angiotensin II type 1 receptor blockers: class effects versus molecular effects. J. Renin-Angiotensin-Aldosterone Syst. JRAAS 12, 1–7. https://doi.org/10.1177/1470320310370852.

Moss, S., Subramanian, V., Acharya, K.R., 2020. Crystal structure of peptide-bound neprilysin reveals key binding interactions. FEBS Lett. 594, 327–336. https://doi.org/10.1002/1873-3468.13602.

Nishimuta, H., Houston, J.B., Galetin, A., 2014. Hepatic, intestinal, renal, and plasma hydrolysis of prodrugs in human, cynomolgus monkey, dog, and rat: implications for in vitro-in vivo extrapolation of clearance of prodrugs. Drug Metab. Dispos. 42, 1522–1531. https://doi.org/10.1124/dmd.114.057372.

PariseFilho, R., Polli, M.C., BarberatoFilho, S., Garcia, M., Ferreira, E.I., 2010. Prodrugs available on the Brazilian pharmaceutical market and their corresponding bioactivation pathways. Brazilian J. Pharma. Sci. 46, 393–420. https://doi.org/10.1590/S1984-82502010000300003.

Patti, R., Sinha, A., Sharma, S., Yoon, T.S., Kupfer, Y., 2019. Losartan-induced Severe Hepatic Injury: A Case Report and Literature Review. Cureus 11, e4769. https://doi.org/10.7759/cureus.4769.

Pinto, Y.M., Paul, M., Ganten, D., 1998. Lessons from rat models of hypertension: from Goldblatt to genetic engineering. Cardiovasc. Res. 39, 77–88. https://doi.org/10.1016/s0008-6363(98)00077-7.

Plant, N., 2004. Strategies for using in vitro screens in drug metabolism. Drug Discov. Today 9, 328–336. https://doi.org/10.1016/s1359-6446(03)03019-8.

Pryde, D.C., Maw, G.N., Planken, S., Platts, M.Y., Sanderson, V., Corless, M., Stobie, A., Barber, C.G., Russell, R., Foster, L., Barker, L., Wayman, C., Van Der Graaf, P., Stacey, P., Morren, D., Kohl, C., Beaumont, K., Coggon, S., Tute, M., 2006. Novel selective inhibitors of neutral endopeptidase for the treatment of female sexual arousal disorder. Synthesis and activity of functionalized glutaramides. J. Med. Chem. 49, 4409–4424. https://doi.org/10.1021/jm060133g.

Pryde, D.C., Cook, A.S., Burring, D.J., Jones, L.H., Foll, S., Platts, M.Y., Sanderson, V., Corless, M., Stobie, A., Middleton, D.S., Foster, L., Barker, L., Van Der Graaf, P., Stacey, P., Kohl, C., Coggon, S., Beaumont, K., 2007. Novel selective inhibitors of neutral endopeptidase for the treatment of female sexual arousal disorder. Bioorg. Med. Chem. 15, 142–159. https://doi.org/10.1016/j.bmc.2006.10.002.

Bhuket, Ratnatilaka Na, P., Jithavech, P., Ongpipattanakul, B., Rojsitthisak, 2019. Interspecies differences in stability kinetics and plasma esterases involved in hydrolytic activation of curcumin diethyl disuccinate, a prodrug of curcumin. RSC Adv. 9, 4626–4634.

Rautio, J., Kumpulainen, H., Heimbach, T., Oliyai, R., Oh, D., Järvinen, T., Savolainen, J., 2008. Prodrugs: design and clinical applications. Nat. Rev. Drug Discov. 7, 255–270. https://doi.org/10.1038/nrd2468.

Richardson, S.J., Bai, A., Kulkarni, A.A., Moghaddam, M.F., 2016. Efficiency in drug discovery: liver S9 fraction assay as a screen for metabolic stability. Drug Metab. Lett. 10, 83–90. https://doi.org/10.2174/1872312810666160223121836.

Ritchie, T.J., Macdonald, S.J., 2009. The impact of aromatic ring count on compound developability–are too many aromatic rings a liability in drug design? Drug Discov. Today 14, 1011–1020. https://doi.org/10.1016/j.drudis.2009.07.014.

Ruf, S., Buning, C., Schreuder, H., Horstick, G., Linz, W., Olpp, T., Pernerstorfer, J., Hiss, K., Kroll, K., Kannt, A., Kohlmann, M., Linz, D., Hübschle, T., Rütten, H., Wirth, K., Schmidt, T., Sadowski, T., 2012. Novel β-amino acid derivatives as inhibitors of cathepsin A. J. Med. Chem. 55, 7636–7649. https://doi.org/10.1021/jm300663n.

Sica, D.A., Gehr, T.W., Ghosh, S., 2005. Clinical pharmacokinetics of losartan. Clin. Pharmacokinet. 44, 797–814. https://doi.org/10.2165/00003088-200544080-00003.

Tao, W., Zhao, D., Sun, M., Wang, Z., Lin, B., Bao, Y., Li, Y., He, Z., Sun, Y., Sun, J., 2018. Intestinal absorption and activation of decitabine amino acid ester prodrugs mediated by peptide transporter PEPT1 and enterocyte enzymes. Int. J. Pharm. 541, 64–71. https://doi.org/10.1016/j.ijpharm.2018.02.033.

Thipparaboina, R., Kumar, D., Chavan, R.B., Shastri, N.R., 2016. Multidrug co-crystals: towards the development of effective therapeutic hybrids. Drug Discov. Today 21, 481–490. https://doi.org/10.1016/j.drudis.2016.02.001.

Wang, D., Zou, L., Jin, Q., Hou, J., Ge, G., Yang, L., 2018. Human carboxylesterases: a comprehensive review. ActapharmaceuticaSinica B 8, 699–712. https://doi.org/10.1016/j.apsb.2018.05.005.

Wang, Y., Thatcher, S.E., Cassis, L.A., 2017. Measuring Blood Pressure Using a Noninvasive Tail Cuff Method in Mice. Methods Mol. Biol. 1614, 69–73. https://doi.org/10.1007/978-1-4939-7030-8_6.

Ward, S.E., Beswick, P., 2014. What does the aromatic ring number mean for drug design? Expert Opin. Drug Discov. 9, 995–1003. https://doi.org/10.1517/17460441.2014.932346.

Weeda, E.R., Coleman, C.I., McHorney, C.A., Crivera, C., Schein, J.R., Sobieraj, D.M., 2016. Impact of once- or twice-daily dosing frequency on adherence to chronic cardiovascular disease medications: A meta-regression analysis. Int. J. Cardiol. 216, 104–109. https://doi.org/10.1016/j.ijcard.2016.04.082.

Williams, E.T., Bacon, J.A., Bender, D.M., Lowinger, J.J., Guo, W.K., Ehsani, M.E., Wang, X., Wang, H., Qian, Y.W., Ruterbories, K.J., Wrighton, S.A., Perkins, E.J., 2011. Characterization of the expression and activity of carboxylesterases 1 and 2 from the beagle dog, cynomolgus monkey, and human. Drug Metab. Dispos. 39, 2305–2313. https://doi.org/10.1124/dmd.111.041335.

Wong, P.C., Price, W.A., Jr, Chiu, A.T., Duncia, J.V., Carini, D.J., Wexler, R.R., Johnson, A.L., Timmermans, P.B., 1990a. Nonpeptide angiotensin II receptor antagonists. XI. Pharmacology of EXP3174: an active metabolite of DuP 753, an orally active antihypertensive agent. J. Pharmacol. Exp. Therapeut. 255, 211–217.

Wong, P.C., Price, W.A., Jr, Chiu, A.T., Duncia, J.V., Carini, D.J., Wexler, R.R., Johnson, A.L., Timmermans, P.B., 1990b. Hypotensive action of DuP 753, an angiotensin II antagonist, in spontaneously hypertensive rats. Nonpeptide angiotensin II receptor antagonists. Hypertension 15 (5), 459–468.

World Health Organization. (WHO). Hypertension, 2019. Available from: https://www.who.int/health-topics/hypertension/#tab=tab_1.

Yasar, U., Forslund-Bergengren, C., Tybring, G., Dorado, P., Llerena, A., Sjöqvist, F., Eliasson, E., Dahl, M.L., 2002. Pharmacokinetics of losartan and its metabolite E-3174 in relation to the CYP2C9 genotype. Clin. Pharmacol. Therapeut. 71, 89–98. https://doi.org/10.1067/mcp.2002.121216.